Novel Type of Two-Impinging-Jets Reactor for Solid–Liquid Enzyme Reactions

Asghar Molaei Dehkordi
Dept. of Chemical and Petroleum Engineering, Sharif University of Technology, Tehran, Iran

DOI 10.1002/aic.10673
Published online September 27, 2005 in Wiley InterScience (www.interscience.wiley.com).

The isomerization of D-glucose to D-fructose using the immobilized glucose isomerase, as a typical model system of solid–liquid enzyme reactions has been carried out in a novel type of two-impinging-jets reactor (TIJR), which is characterized by a rotating inner cylinder in a stationary one. Because of the impinging process, turbulence, and complex trajectory of the solid particles within the reactor, the fractional conversion of glucose obtained in the TIJR increased dramatically compared to that obtained by conventional reaction systems. A compartment model was considered to describe the pattern of flow [residence time distribution (RTD) of solid particles] within the TIJR. Considering such a flow pattern, a stochastic model for the RTD of the solid particles was developed using Markov chains models. The latter was correlated with the experimental RTD data, obtained by using a tracer analysis technique. © 2005 American Institute of Chemical Engineers *AIChE J,* 52: 692–704, 2006
Keywords: impinging jets, opposed jets, glucose isomerase, enzymatic isomerization, residence time distribution

Introduction

Solid–liquid enzyme reactions constitute important processes in biochemical industries. Among the latter, the isomerization of glucose to fructose is one of the most widely used processes in the food industry in producing dietetic "light" foods and drinks because it improves the sweetening, color, and hygroscopic characteristics in addition to reducing viscosity. Also, fructose is about 75% sweeter than sucrose, is absorbed more slowly than glucose, and is metabolized without the intervention of insulin. For all these reasons, this process is widely studied both with cells and with enzymes, both free and immobilized (IE).[1-13] From the perspective of chemical kinetics, isomerization of glucose to fructose is a reversible reaction, with an equilibrium constant of approximately unity at 55°C.[14] The heat of reaction is on the order of 5 kJ/mol[14] and, consequently, the equilibrium product contains roughly a 1:1 ratio of glucose to fructose that does not change appreciably with temperature, such that at 55°C the fructose content at equilibrium is 50%, and at higher temperatures such as 60, 70, 80, and 90°C is 50.7, 52.5, 53.9, and 55.6%, respectively. However, increasing temperature decreases stability and the enzyme half-life and therefore productivity. Most industrial plants run at 58–60°C, a temperature with low risk for microbial contamination.

The process was originally carried out in batch reactors with soluble enzymes. It was later extended to one involving immobilized glucose isomerase (IGI), which is of interest to us in the present work. In addition to the aforementioned batch reactors, there are various types of enzyme reactors, including continuous stirred tank reactors (CSTR), fixed-bed reactors, simulated moving beds, and fluidized-bed reactors. In the fixed- and fluidized-bed reactors, the enzymes are immobilized in the pores of microporous particles, which can take various shapes such as cylindrical. Because the microporous particles provide a large surface area for the reactions, and packing the particles in a tubular reactor is straightforward, tubular packed-bed reactors consisting of IGI are widely used nowadays. Thus isomerization of glucose to fructose is normally carried out in multiple tubular packed-bed reactors in parallel lines with an isomerization time ranging from 0.5 to 4 h.[14]

Correspondence concerning this article should be addressed to A. M. Dehkordi at amolaeid@sharif.edu.

The impinging jets (IJ) technique is a unique flow configuration. The first patent for this technique was probably published by Carver and coworkers.[15] The IJ technique was used by Elperin for gas–solid suspensions[16] and further developed by Tamir in various chemical engineering processes.[17] In addition, Mujumdar and coworkers conducted extensive investigations on the modeling and application of IJ technique in heat-transfer processes.[18-21] The method provides a powerful technique for intensifying transfer processes. The principle of IJ is to bring the two jets flowing along the same axis in the opposite direction into collision. As the result of such a collision, a relatively narrow zone, called the impingement zone of high turbulence intensity, is created, which offers excellent conditions for intensifying heat- and mass-transfer rates. The IJ technique has been successfully applied to the absorption and desorption of gases[22-26]; dissolution of solids[27]; drying of solids[28-32]; dust collection[33]; absorption with chemical reaction[34,35]; two-liquid phase reaction[36]; mixing[37-40]; evaporative cooling of air[41]; bioreactions[42,43]; liquid–liquid extraction[44-46]; metal extraction and stripping processes[47,48]; liquid–liquid extraction with chemical reaction[49,50]; crystallization; and precipitation.[51-53] The main objectives of the present study were (1) to investigate the pertinent parameters on the hydrodynamic behavior of the proposed reactor, and modeling of the residence time distribution of solid particles in the reactor through the Markov chains models; and (2) to evaluate the performance capability of a novel type of two-impinging-jets reactor for solid–liquid enzyme reactions using glucose isomerization as a typical model system.

Reaction Kinetics

We briefly introduce glucose–fructose enzymatic isomerization, which is a reversible reaction, and is normally given by the following expression:

$$G + E \underset{k_g}{\overset{k_{-g}}{\rightleftharpoons}} X \underset{k_{-f}}{\overset{k_f}{\rightleftharpoons}} F + E \tag{1}$$

where G, E, and F represent glucose, the enzyme, and fructose, respectively, whereas X is an intermediate complex formed during the reaction.

According to the Briggs–Haldane kinetic model the reaction rate R is given by[54,55]

$$R = \frac{k_{-g}k_f[G] - k_g k_{-f}[F]}{k_g + k_f + k_{-g}[G] + k_{-f}[F]} \tag{2}$$

$$[E_t] = \frac{v_{mf}K_{mr}[G] - v_{mr}K_{mf}[F]}{K_{mf}K_{mr} + K_{mr}[G] + K_{mf}[F]} \tag{3}$$

where $[G]$, $[E_t]$, $[F]$, and $[X]$ denote the concentrations of glucose, enzyme, fructose, and the intermediate complex, respectively, and

$$v_{mf} = k_f[E_t] \qquad v_{mr} = k_g[E_t] \qquad K_{mf} = \frac{k_g + k_f}{k_{-g}} \qquad K_{mr} = \frac{k_g + k_f}{k_{-f}} \tag{4}$$

Moreover, K_{mf} and v_{mf} are called the Michaelis–Menten constant and maximum velocity for the forward reactions, respectively, whereas K_{mr} and v_{mr} are the similar quantities for the reverse reactions. The relation between the equilibrium concentrations of glucose and fructose, $[G_e]$ and $[F_e]$, respectively, is given by

$$[G_0] = [G] + [F] = [G_e] + [F_e] = (1 + K_e)[G_e] = (1 + K_e^{-1})[F_e] \tag{5}$$

where $[G_0]$ is the initial concentration of glucose and the equilibrium constant is given by

$$K_e = \frac{[F_e]}{[G_e]} = \frac{v_{mf}K_{mr}}{v_{mr}K_{mf}} \tag{6}$$

The reaction rate R is normally given in terms of the Michaelis–Menten constants. So, if $[\Delta G] = [G] - [G_e]$, then

$$R = \frac{v_m[\Delta G]}{K_m + [\Delta G]} \tag{7}$$

with

$$v_m = \frac{K_{mr}v_{mf}(1 + K_e^{-1})}{K_{mr} - K_{mf}} \tag{8}$$

$$K_m = \frac{K_{mf}K_{mr}}{K_{mr} - K_{mf}}\left[1 + (K_{mf}^{-1} + K_eK_{mr}^{-1})\frac{[G_0]}{1 + K_e}\right] \tag{9}$$

The following correlations have been reported for D-glucose isomerization using Sweetzyme type T® immobilized enzyme, which satisfactorily fit experimental data concerning the reaction[56]:

$$K_e = 4.12 \times 10^{-2}\exp(1022/T) \tag{10}$$

$$k_{-f}[E_t] = 1.7 \times 10^{11}\exp(-10{,}000/T) \quad \text{mol kg}^{-1}\,\text{s}^{-1} \tag{11}$$

$$k_{-g}[E_t] = 7.2 \times 10^{9}\exp(-9200/T) \quad \text{mol kg}^{-1}\,\text{s}^{-1} \tag{12}$$

$$k_f[E_t] = k_g[E_t] = 7.7 \times 10^{3}\exp(-6300/T) \quad \text{m}^3\,\text{kg}^{-1}\,\text{s}^{-1} \tag{13}$$

where T is temperature in K.

Experimental Studies

Chemicals

All chemicals used in the present study were of analytical grade; D-glucose in crystalline form was provided by Merck Co. (Darmstadt, Germany). The immobilized enzyme, Sweetzyme T® (E.C. 5.3.1.5, D-xylose ketolisomerase) was provided as a gift from Novo Nordisk (Bagsværd, Denmark). The IGI enzyme particles were of cylindrical shape with 0.3 to 1 mm diameter, 1 to 1.5 mm length, and particle density of 1.43 g

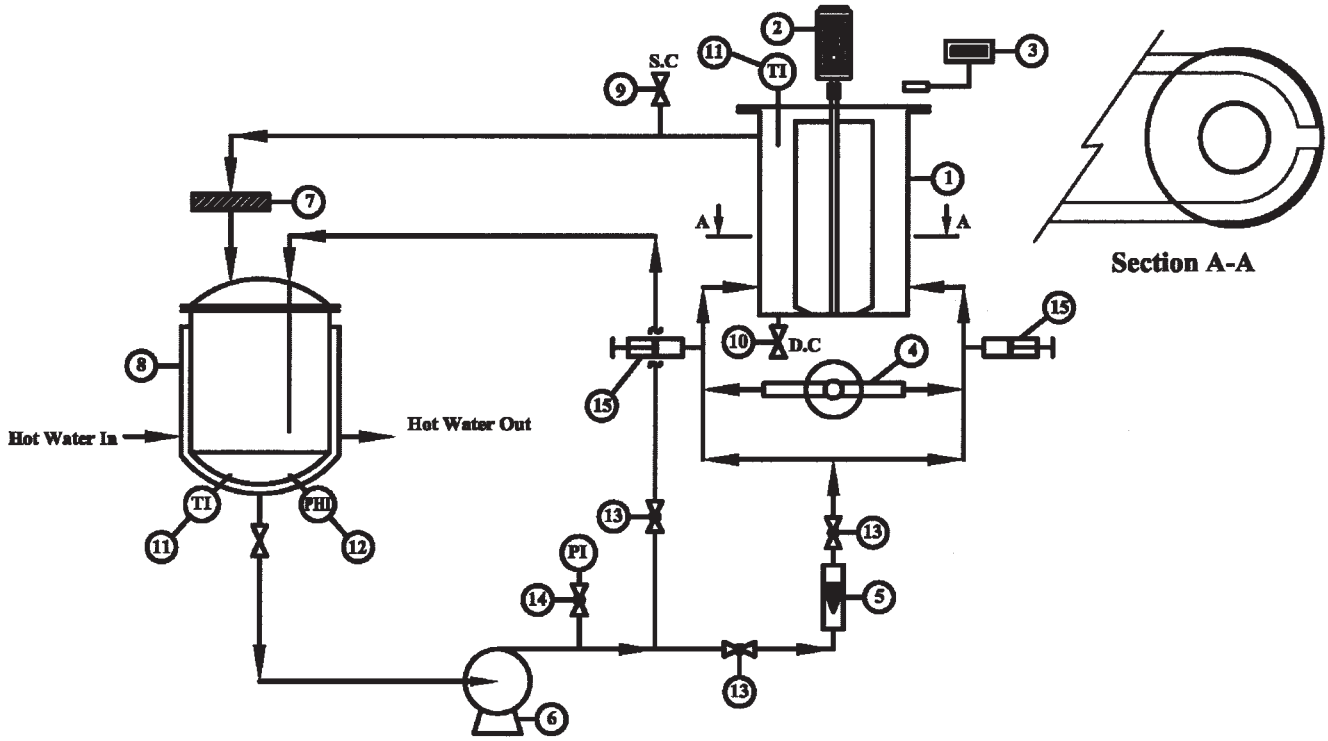

Figure 1. Experimental setup.

(1) Reactor system; (2) variable-speed electric motor; (3) digital tachometer; (4) solid enzyme feeder; (5) substrate solution rotameter; (6) substrate centrifugal pump; (7) filter; (8) jacketed feed vessel; (9) sampling connection (SC); (10) drain connection (DC); (11) temperature indicator (TI); (12) pH meter (PHI); (13) globe valves; (14) pressure indicator (PI); and (15) syringes.

cm^{-3}. The dry specific activity of the enzyme was reported to be 350 IGIU/g by the manufacturer.

Method of analysis

Determination of the glucose concentration was carried out using a glucose oxidase/peroxidase method described by Coburn and Carrol.[57] The concentration of fructose during the course of the D-glucose converting to D-fructose was measured by the cysteine–carbazole method.[58] The accuracy of the above-mentioned analytical methods was examined using known samples of D-glucose and D-fructose solutions. From these tests, the errors of the analytical methods were found to be within the range of $\pm 3.5\%$.

Experimental apparatus

The flow diagram of the experimental setup, shown in Figure 1, consisted of the following parts: (1) reactor system composed of two coaxial cylinders (inner and outer), which are fully described in the following section; (2) a variable-speed electric motor to investigate the influence of the inner rotating cylinder speed [Taylor number (Ta)] on the conversion of glucose to fructose and hydrodynamics behavior of the proposed reactor. Note that in the present investigation only the inner cylinder was rotated and the outer cylinder was fixed. The substrate (D-glucose solution) and the solid enzyme particles were introduced into the annular space of the reactor by acceleration pipes (see Figure 2). Thus, the main contact between the substrate and the enzyme took place between the inner rotating cylinder and the outer stationary one (annular gap). A description of other parts of the experimental setup is given in the Figure 1 caption.

TIJ reactor

The schematic diagram (cross–sectional top view) of the TIJ reactor, including IGI enzyme feeder, substrate acceleration pipes, and the bottom cross-sectional view of the reactor, is illustrated in Figure 2. Considering Figure 1, the reactor setup was composed of an outer fixed cylinder made of Pyrex® glass with 7 cm ID and 20 cm working height, and an inner rotating cylinder made of polypropylene with 5 cm OD, creating an annular space and vortex flow. A stainless steel shaft is positioned throughout the inner rotating cylinder to increase the system inertia and reduce wobbling. The main aims of the inner rotating cylinder are: (1) to keep the solid particles in suspension; (2) to create turbulence and vortex flow similar to that of a Taylor–Couette flow device; and (3) to increase the mean residence time of the solid particles arising from complex flow pattern created in such a device. On the other hand, the agitation promoted by the inner rotating cylinder is less aggressive than that obtained with conventional stirrers. The latter is an important feature when sensitive particles are present in the reaction medium. In addition to the advantage of using the impinging-jets technique, the two-impinging-jets reactor (TIJR) has the advantage of possessing one extra operating variable: the rotation of the inner cylinder as well. The latter may be used to keep the particles in suspension for low axial flows (low axial Reynolds number), a difficult task in conventional fluidized-bed reactors. The IGI particles were added to

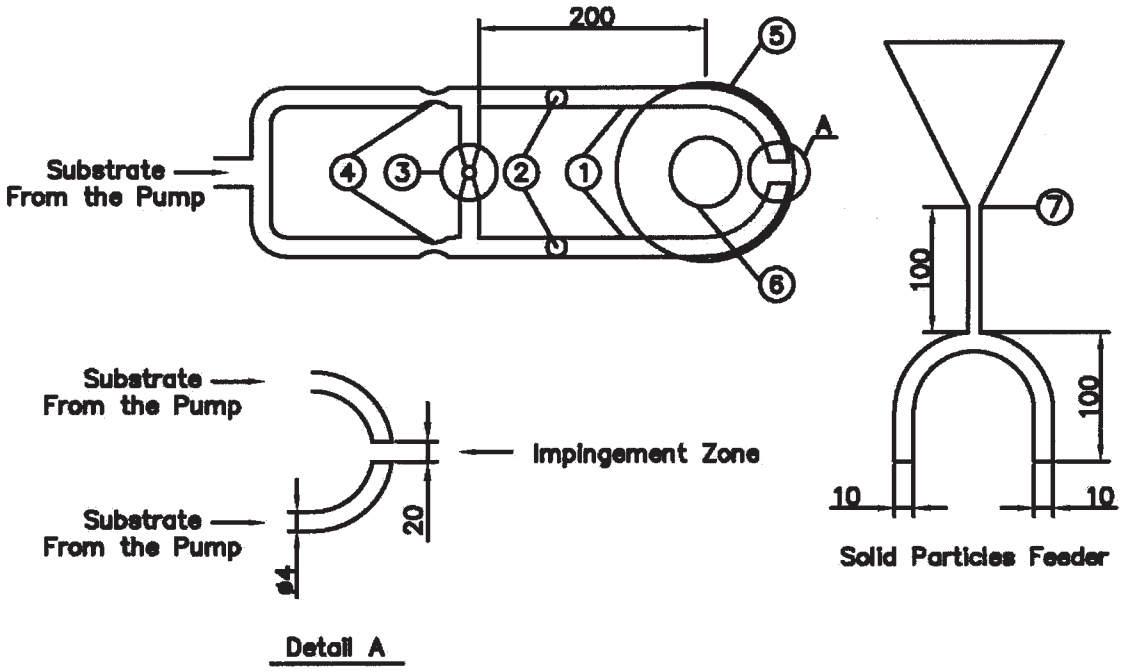

Figure 2. Diagram (cross-sectional top view) of the TIJR and solid particles feeder.

(1) Acceleration pipes; (2) syringes; (3), (7) solid particles feeder; (4) contraction; (5) outer cylinder; (6) inner cylinder. All dimensions are in millimeters.

the two liquid streams through a hopper-type feeder shown in Figure 2. To provide the desired mass flow rate of the IGI particles, the exit size of the feeder could be varied. As shown in Figure 2 the two suspension streams (the substrate solution and IGI enzyme particles) were fed through acceleration pipes made of Pyrex® glass. The accelerated suspension streams impinged at the annular space (see Figure 2) and moved along the inner rotating cylinder to the outlet port of the reactor through a complex trajectory (see Figure 1).

Experimental procedure

The D-glucose feed was prepared by dissolving the necessary quantity of D-glucose in a solution of $MgSO_4 \cdot 7H_2O$ of 0.55 kg m^{-3} to stabilize the enzyme, and the pH of the solution was adjusted to 7.5 with a 100 mol m^{-3} solution of sodium carbonate. Because oxygen in the syrup inactivates the enzyme and is responsible for increased formation of secondary products during isomerization, a low oxygen tension thus has to be achieved by adding sodium metabisulfite ($Na_2S_2O_5$) of 2 mol m^{-3}. The temperature of the feed solution was increased to 60°C by means of hot water feeding into the jacket and total circulation of the content of the feed vessel by means of the feed pump.

In each experimental run, the inner rotating cylinder speed was adjusted at the desired value (checked by a digital tachometer) and then the substrate solution and the solid enzyme were continuously fed to the reaction system at given volumetric- and mass-flow rates, respectively. The solution-flow rate was regulated using the globe valve and rotameter and the mass-flow rates of the enzyme could be adjusted by varying the size of the feeder device (see Figure 2). A recycled stream from the discharge of the feed pump was used to homogenize the entire content of the feed vessel. The effluent, after being passed through a filter to separate the spent enzyme, was recycled to the feed vessel. The samples were taken both through the sampling connection (SC) and the feed vessel for the measurement with a syringe. Analysis of the samples was performed by the aforementioned analytical methods for the glucose–fructose concentrations.

For each data point, the experimental run was repeated at least three times, and thus each data point was determined based on the mean value of at least three measurements of outlet concentrations with a standard deviation of 2–4%.

Results and Discussion

The operating conditions for the determination of glucose conversion and the residence time distribution of the solid particles were as follows:

- Taylor number, Ta: 12,466–31,167
- Axial Reynolds number, Re_{ax}: 188–1880
- The solid enzyme mass flow rate, W_s: 1 to 4 g/s
- Temperature within the reactor, T: about 60°C
- Concentration of glucose solution, $[G_0]$: 0.1 kmol/m^3
- Volumetric flow rate of glucose solution: 1–10 dm^3/min

Evaluation of performance capability of the TIJR

To compare the performance capability of the TIJR compared with that of other reactor types, a number of experiments were carried out by using a laboratory-scale batch stirred tank reactor (BSTR) equipped with a turbine-type impeller and a laboratory jacketed packed-bed reactor (PBR) with the same conditions used in the TIJR. The PBR was a glass tube with 12 mm ID and 145 mm working height. The PBR was filled with

Table 1. Fractional Conversion (%) of D-Glucose in Various Kinds of Reactors

Mean Residence Time (s)	Reactor Types			
	BSTR	PBR	DJR[59]	TIJR
60	2	10	2.5	37
120	3	15	12	50

5 g catalyst. The liquid holdup within the PBR was experimentally determined to be 7.3 cm^3. The temperature of the PBR was controlled by introducing hot water into its jacket. According to these experiments, the performance capability of the TIJR compared with that of the conventional BSTR and PBR is evaluated on the basis of Table 1, which contains data for the fractional conversion of D-glucose vs. mean residence time as well as the data reported to be obtained by using a downflow jet loop reactor (DJR).[59] It may be concluded from these data that the TIJR is superior to conventional reactors. Although the power input to the TIJR is higher than that to PBRs, its performance capability is much higher than that of PBRs. However, in most cases high-performance systems require a high energy input. One explanation for such a high fractional conversion obtained in the TIJR may be as follows: the external mass-transfer resistance surrounding the solid particles (interphase mass-transfer resistance), arising from the complex flow pattern, strong collision of the jets, higher shearing forces acting on the particles, and high velocity of the solid particles within the reaction compartment especially at the impingement zone could be eliminated. In addition, these experimental results clearly indicate that the performance capability of the conventional reaction systems was severely affected by external mass-transfer limitations.

Mean residence time

Measurement of the mean residence time of the liquid and the solid phases in the reaction system requires knowledge of the liquid and solid holdups within the reactor, respectively. One of the most widely used techniques for the holdup estimation in various types of reactors is the shutdown procedure. To determine the solid and liquid holdups within the reactor, vegetable grains (millet seeds) as solid particles and water as the liquid solution were used. Because there are certain similarities between the solid enzyme and millet seed, such as density and apparent shape, millet seeds were selected as the solid particles.

According to the shutdown procedure, water and vegetable grains were introduced continuously at the given volumetric- and mass-flow rates, respectively, into the reactor. After the steady-state condition was established, the flow of the water and the grains was suddenly ceased. The materials remaining in the reactor were collected at the drain port (DC). The weight of millet seeds (after drying) and the liquid-phase volume were measured.

Influence of Liquid Flow Rate (Axial Reynolds Number, Re_{ax}*).* Figure 3 shows the plot of the solid holdup as a function of the liquid flow rate with the solid mass flow rate as a parameter at the fixed Taylor number (Ta) = 12,466. As may be observed, at a given solid mass flow rate, increasing the liquid flow rate (axial Reynolds number) decreases the solid holdup in the reactor. This behavior is expected and can be explained by an increase in the axial mean velocity, which should promote the chance of solid particles being washed out of the reaction system. It should be noted that the axial Reynolds number and Taylor number are normally given by the following expressions in such a reactor:

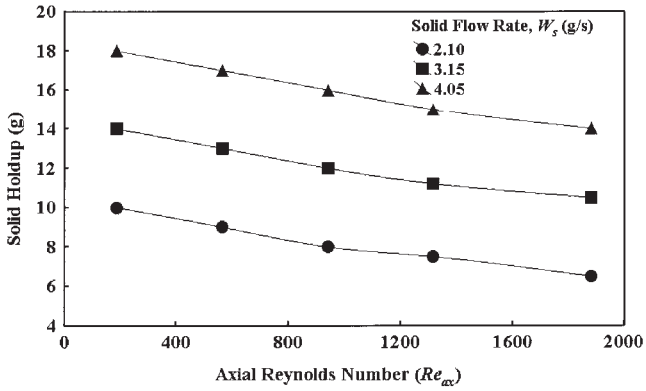

Figure 3. Effect of axial Reynolds number (Re_{ax}) on the solid holdup.

Taylor number (Ta) = 12,466.

$$\mathrm{Re}_{ax} = \frac{U_{ax} d}{\nu} \tag{14}$$

$$\mathrm{Ta} = \frac{2\pi R_i \omega d}{\nu}\left(\frac{d}{R_i}\right)^{1/2} \tag{15}$$

where U_{ax}, d, ν, R_i, and ω are the mean axial velocity, angular gap width ($=R_o - R_i$), kinematic viscosity, inner rotating cylinder radius, and inner rotating cylinder speed, respectively; and R_o is the outer radius of the annular gap.

Figure 4 shows the plot of liquid holdup as a function of the solid mass flow rate with the axial Reynolds number as a parameter at the fixed Taylor number, 12,466. It is apparent that at a given axial Reynolds number and Taylor number the holdup of the liquid phase in the reactor is nearly constant and insensitive to the change in the solid mass flow rate. Such a behavior can be explained by noting that the flow rate of liquid

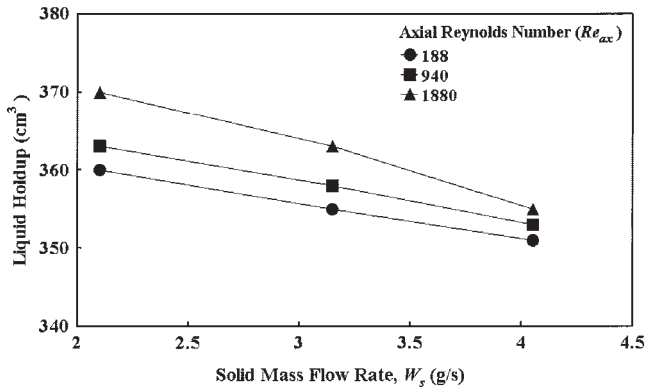

Figure 4. Effect of solid mass flow rate (W_s) on the liquid holdup.

Ta = 12,466.

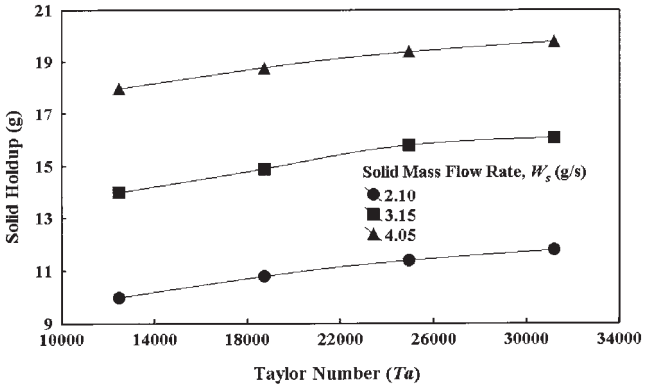

Figure 5. Effect of Taylor number (Ta) on the solid holdup.

Re_{ax} = 188.

in all experimental runs was much greater than that of solid. Thus, variation in the solid mass flow rate may not have a profound influence on the liquid holdup.

Influence of Taylor Number (Ta). Figure 5 illustrates the solid holdup as a function of the Taylor number with the solid mass flow rate (W_s) as a parameter at the fixed axial Reynolds number, 188. As may be observed the solid holdup increases slowly with an increase in the Taylor number at a fixed axial Reynolds number. This can be explained as follows: an increase in the Taylor number causes the intravortex mixing to become more effective, the flow pattern becomes more complicated, and there is an increase in the helical waving vortices.[60] On the other hand, this behavior can be explained by an increase in the interparticle collisions and collisions with the reactor system walls and thus the chance of solid particles leaving the reactor is reduced.

It should be added that the effect of Ta number was investigated at the other Re_{ax} numbers. According to the experimental results obtained, the latter illustrated similar trends like that in Figure 5, and thus it was decided to include only the experimental results at Re_{ax} = 188.

Influence of Solid to Liquid Mass Flow Ratio. Figure 6 shows a plot of variations of the ratio of solid mean residence time to liquid mean residence time vs. the solid to liquid mass flow rate ratio, with the solid mass flow rate as a parameter. It is shown in this figure that at a given solid mass flow rate, the mean residence time ratio decreases with increasing mass flow rate ratio. This behavior can be explained by considering that an increase in the liquid flow rate decreases the liquid mean residence time with an inverse proportion, whereas such an increase in the liquid flow rate has no profound effect on the solid holdup (see Figure 3): that is, a tenfold change in the liquid flow rate decreases the solid mean residence time by only 23%. It should be added that, according to the definition, the ratio of the mean residence times is proportional to the reciprocal of the mass-flow rates times the ratio of the solid holdup to liquid holdup in mass units given by

$$\frac{\bar{t}_s}{\bar{t}_l} = \frac{\psi_s}{\psi_l}\left(\frac{W_l}{W_s}\right) \tag{16}$$

where ψ_s, ψ_l, W_s, and W_l are the solid holdup, liquid holdup (mass), solid mass-flow rate, and liquid mass-flow rate, respectively.

Residence time distribution (RTD) of solid particles

To gain an insight into the behavior of solid particles in the TIJR, RTD experiments were conducted. The latter is an important parameter because of (1) oscillatory motion of the particles at the impingement zone formed at a plane in which the two jets collide with each other, which might cause internal recirculation and affect the mean residence time in the reactor; and (2) complex flow pattern of solid particles within the reaction chamber. However, the determination of the solid particle RTD is normally encountered with major difficulties. The latter is explained by the discontinuous flow of solid particles and the mean residence time of solid particles in the reactor, which is only a few seconds, and thus the tracer must be injected into the system during very short injection times if one wants to obtain a true impulse response and useful information.

The number of solid particles flowing through the TIJR is on the order of 10^3 particles per second for a typical mass flow rate of 5 g/s compared to 10^6 particles per second in a continuous flow of particles.[17] Consequently, only a small number of tagged particles could be used in tracer experiments without disturbing the flow conditions. In the present study, 200 painted millet seeds were applied as the tracer.

Under such conditions, the behavior of the solid particles is highly discontinuous with respect to the length of the observed phenomena. Only random fluctuations of single particles could be detected, and the reproducibility of the results becomes unlikely.[17] Therefore, an average behavior should be determined. Thus, a number of repetitive experiments and statistical averaging is required. The mean concentration (C_m) at a certain time, reflecting average behavior under conditions of practical use, is calculated by

$$C_m = \frac{1}{m}\sum_{i=1}^{m} C_i \tag{17}$$

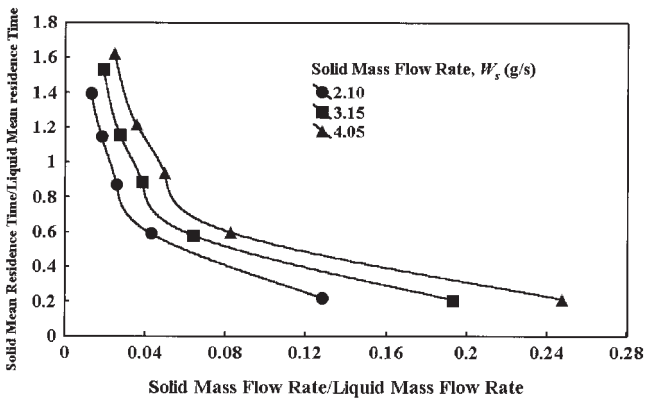

Figure 6. Variation of the ratio of solid to liquid mean residence time within the TIJR.

Ta = 12,466.

where C_i is the number of painted particles (or concentration) corresponding to a specific experiment i and m is the number of repetitive experiments. As can be easily realized, the latter involves repetitive experiments and statistical averaging, all of which lead to considerable amounts of experimental work and time. However, a more applicable technique is to take a cumulative reading of the response of each experiment instead of instantaneous reading (mixed cup). Each reading was collected during a time interval Δt. When Δt is increased from zero to some higher values, the sensitivity of reading decreases until at a certain value of Δt, the random fluctuations of particles are no longer observed. The only remaining problem is the determination of the correct value for Δt to use in experiments because Δt should be large enough to eliminate any random fluctuation but not so large that useful information is lost.

As an outcome of the aforementioned facts, a measuring device, like that developed by Tamir and coworkers, has been used.[17] The device is a circular plate divided into 24 segments. The circular plate was placed under the effluent port of the reactor and was driven at the desired rotation speeds by means of a variable-speed electric motor. The speed of the latter was checked by a digital tachometer. Thus, different sampling intervals were obtained by changing the speed of the electric motor. The problem is how to obtain the true RTD curve, where the true RTD curve is the one obtained from a representative population of particles in which random oscillation arising from the individual behavior of a single particle is no longer felt as previously discussed.

To overcome the above-mentioned difficulty, a stochastic model for the RTD in the reactor was developed based on the flow pattern first proposed by Van de Vuss.[61] When the experimental results were correlated with the theoretical model, the true RTD curve was determined.[17] Because the collision of the particles in the impinging zone is a stochastic phenomenon, a suitable mathematical technique to handle such a process could be Markov chains models.[17] An additional reason for applying the latter is the discrete-time process in the reactor as well as the measuring device used for the RTD of the solid particles. Some aspects of the discrete-time Markov chains are described below.

According to the discrete-time Markov chains, the probability of an event at time $t + 1$ ($t = 0, 1, 2, \cdots$) is not dependent on the state history before time t. Thus, the values of the state probability of the system at the given time t determine the conditional properties for future values of the system. These values are called the state probabilities of the system, which are the transition probabilities between state i and j designated by p_{ij} in one step (one time interval). The latter is time independent. These one-step state transition probabilities are displayed in the one-step transition probability matrix ($\mathbf{P} = [p_{ij}]$). The latter is an $N \times N$ matrix, where N is the number of possible states that the system may occupy. The rows of matrix $\mathbf{P}$ consist of the probabilities of all possible transitions from a given state (i) to the others, and so sum to unity.

$$\sum_{j=1}^{N} p_{ij} = 1 \tag{18}$$

Other definitions and relations regarding to Markov processes are as follows:

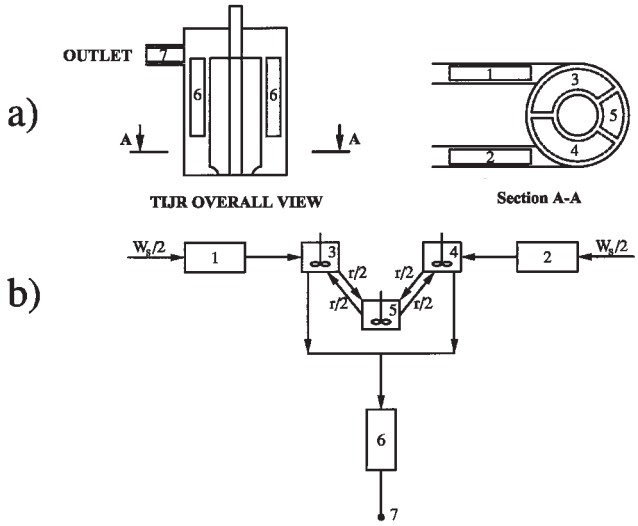

Figure 7. Model of the TIJR.

(a) Flow regions proposed for the reactor; (b) The resulting model; 1, 2, 6: perfect plug regions; 3, 4, 5: perfect mixed regions.

- $s_i(n)$, the state probability, defined as the probability that the system will be in the state i after n transition from a given starting point, which is time dependent.
- $\mathbf{S}(n)$, the state probability vector, a row vector composed of the elements $s_i(n)$ and $\mathbf{S}(n) = [s_1(n), s_2(n), \ldots, s_N(n)]$.
- $\mathbf{S}(0)$, initial state probability vector, $\mathbf{S}(0) = [s_1(0), s_2(0), \ldots, s_N(0)]$, which is also a known vector in a given system.

According to the Markov processes, the total probability of the system reaching one of all possible N states that can be occupied after n transitions is equal to unity as shown below:

$$\sum_{i=1}^{N} s_i(n) = 1 \tag{19}$$

In addition, the probability that the system is in state j after $n + 1$ transitions is equal to the sum of its probabilities of being in any state i after n transitions, multiplied by the probability of transferring from state i to state j in one transition step, as given by

$$s_j(n + 1) = \sum_{i=1}^{N} s_i(n) p_{ij} \qquad n = 0, 1, 2, \ldots \tag{20}$$

The latter may be displayed in the matrix notation as follows:

$$\mathbf{S}(n + 1) = \mathbf{S}(n) \cdot \mathbf{P} \tag{21}$$

Further details of Markov chains models can be found elsewhere.[17]

Based on the Markov chains models, the reaction system was divided into six regions with equal volumes, depicted in Figure 7. Each region represents a state in the Markov chains model and thus the transition probability p_{ij} is the probability of

a solid particle leaving region i and entering region j. In addition each region was assumed to be an ideal plug flow and/or perfect mixed reactor. Because of countercurrent flows in the impingement zone, a recycle stream r was also considered.[17] Regarding the flow pattern supposed for the TIJR, whenever a solid particle reaches region 6, it leaves the reaction system to state 7 where it remains. Thus, state 7 is a trapping state. The $s_6(n)$ indicates the probability that a solid particle entering the system at $n = 0$ will leave the system after $n\Delta t$ ($n = 1, 2, 3, \cdots$). Consequently, the numerical values of $s_6(n)$ for $n = 0, 1, 2, \cdots$ represent the impulse response of the system after n time intervals Δt. Based on the flow pattern supposed for the TIJR, the transition probability matrix becomes

$$\mathbf{P} = \begin{bmatrix} p_{11} & p_{12} & p_{13} & p_{14} & p_{15} & p_{16} & p_{17} \\ p_{21} & p_{22} & p_{23} & p_{24} & p_{25} & p_{26} & p_{27} \\ p_{31} & p_{32} & p_{33} & p_{34} & p_{35} & p_{36} & p_{37} \\ p_{41} & p_{42} & p_{43} & p_{44} & p_{45} & p_{46} & p_{47} \\ p_{51} & p_{52} & p_{53} & p_{54} & p_{55} & p_{56} & p_{57} \\ p_{61} & p_{62} & p_{63} & p_{64} & p_{65} & p_{66} & p_{67} \\ p_{71} & p_{72} & p_{73} & p_{74} & p_{75} & p_{76} & p_{77} \end{bmatrix} \tag{22}$$

or

$$\mathbf{P} = \begin{bmatrix} 0 & 0 & 1 & 0 & 0 & 0 & 0 \\ 0 & 0 & 0 & 1 & 0 & 0 & 0 \\ 0 & 0 & e^{\alpha} & 0 & r_r(1-e^{\alpha})/(1+r_r) & (1-e^{\alpha})/(1+r_r) & 0 \\ 0 & 0 & 0 & e^{\alpha} & r_r(1-e^{\alpha})/(1+r_r) & (1-e^{\alpha})/(1+r_r) & 0 \\ 0 & 0 & (1-e^{\beta})/2 & (1-e^{\beta})/2 & e^{\beta} & 0 & 0 \\ 0 & 0 & 0 & 0 & 0 & 0 & 1 \\ 0 & 0 & 0 & 0 & 0 & 0 & 1 \end{bmatrix} \tag{23}$$

with

$$\alpha = -n_v(1 + r_r)\Delta\theta/2 \tag{24}$$

$$\beta = -n_v r_r \Delta\theta \tag{25}$$

$$r_r = r/W_s \tag{26}$$

$$\Delta\theta = \Delta t/t_m \tag{27}$$

where n_v and r are the number of vessels in the model and the recycle streams flow rate, respectively. In the above matrix, the diagonal elements p_{jj} are the probabilities that a solid particle remains in the same region (state), the columns vector elements are the probabilities of entering region (state) j, and the row vector elements are the probabilities of leaving region (state) j. The initial state probability vector $\mathbf{S}(0)$ is also known:

$$\mathbf{S}(0) = [s_1(0), s_2(0), s_3(0), s_4(0), s_5(0), s_6(0), s_7(0)] = [0.5, 0.5, 0, 0, 0, 0, 0] \tag{28}$$

In each experimental run, water and solid particles were passed continuously through the reactor. At a certain time ($t = 0$), 200 painted millet seeds were rapidly injected into the solid flow and the number of painted seeds remaining in each segment of the circular plate during the time interval Δt was measured. A number of experiments for the determination of RTD were conducted by varying the time interval Δt from 0.3 to 1 s. From the experimental runs, the mean residence time t_m and the mean square deviation or variance σ^2 were calculated using the following expressions:

$$t_m = \frac{\sum_{i=1}^{24} t_i C_i \Delta t_i}{\sum_{i=1}^{24} C_i \Delta t_i} \tag{29}$$

$$\sigma^2 = \frac{\sum_{i=1}^{24} (t_i - t_m)^2 C_i \Delta t_i}{\sum_{i=1}^{24} C_i \Delta t_i} \tag{30}$$

where Δt_i and C_i are the time interval between two successive segments on the rotating circular plate (a constant value for a fixed rotating speed of circular plate, Δt), and the number of painted seeds in segment i. Because the total number of segments of the circular plate was 24, the upper bound of the above summation is therefore 24.

In the present investigation, the true RTD curve was assumed to be that particular curve having a variance and a mean residence time identical to those of the theoretical model, that is,

$$\sigma^2_{exp} = \sigma^2_{mod} \tag{31}$$

$$(t_m)_{exp} = (t_m)_{mod} \tag{32}$$

The variance of the theoretical RTD curve was determined from

$$\sigma^2_{mod} = \sum_{i=1}^{24} s_6(i)[t_m(i\Delta\theta - 1)]^2 \tag{33}$$

The dimensionless time ($\Delta\theta$) was determined by considering the implication of equality of the two mean residence times of the experimental and theoretical RTD curves; that is,

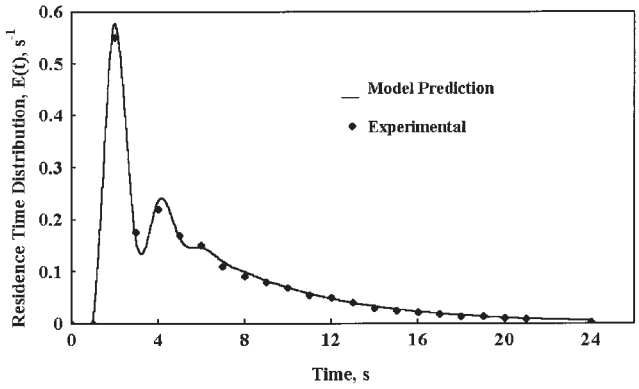

Figure 8. Comparison between the experimental and theoretical solid RTD in the TIJR.

Each increment in the x-axis represents $\Delta t = 0.5$ s; recycle ratio (r_r) = 1.46; variance of the experimental data (σ^2) = 5.26 s^2.

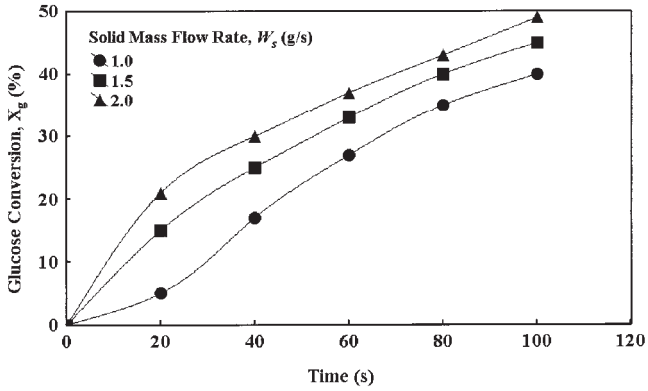

Figure 9. Effect of solid mass flow rate W_s on the fractional conversion of D-glucose to D-fructose in the TIJR.

Re_{ax} = 1880; Ta = 12,466; standard deviations of the data points are between 1.3 and 1.5.

$$1 = \Delta\theta \sum_{i=1}^{24} i s_6(i) \tag{34}$$

where $\Delta\theta$ is defined by Eq. 27.

The procedure in finding the true RTD curve from the experiments is as follows:

(1) The variance and mean residence time are determined from the experimental results and calculated by Eqs. 29 and 30 where the experimental $\Delta t = \Delta t_i$ is recorded.

(2) The dimensionless quantity $\Delta\theta = (\Delta t/t_m)_{exp}$ is obtained from the experimental measurements and operating conditions.

(3) The appropriate value of r_r is the one that satisfies Eq. 34.

(4) We now calculate σ^2_{mod} from Eq. 33 and the procedure is terminated whenever the condition expressed by Eq. 31 is satisfied within the experimental accuracy. Thus, the appropriate pair of the parameters r_r and $\Delta\theta$ is fixed, which yields the true RTD curve.

The book by Tamir,[62] which is an excellent and in-depth source of information on Markov chains models, can help one to apply or extend the method. The above procedure revealed that the best correlation existed with Δt and r_r equal to 0.5 s and 1.46, respectively (Figure 8).

Isomerization of D-glucose to D-fructose

A number of experimental runs have been conducted according to the experimental procedure discussed earlier. The range of the IGI mass-flow rate (W_s) was 1 to 2 g/s and the other certain pertinent parameters were as stated in the experimental procedure section and the operating conditions. Figures 9 and 10 show the obtained experimental results. Figure 9 illustrates the variations of the fractional conversion of D-glucose to D-fructose vs. time with the IGI mass-flow rate W_s as a parameter at Re_{ax} = 1880 and Ta = 12,466. Figure 10, on the other hand, represents the dependency of the fractional conversion of D-glucose to D-fructose on the Taylor number (Ta). As may be observed, some unexpected results have been obtained from the TIJR system. These figures show that a fractional conversion of about 50% (almost equilibrium conditions) was achieved within 100 s, whereas such a fractional conversion has been reported to be obtained in 27 h in a CSTR reactor at 60°C,[63] and a fractional conversion of only 5% has been reported to be obtained in 4 min in a laboratory-scale tubular reactor.[43] In addition, the isomerization time in the industrial-scale plants is in the range of 0.5 to 4 h.[14] The explanations for such a behavior may be as follows:

(1) The external mass-transfer resistance surrounding the solid particles (interphase mass-transfer resistance) highly depends on the particle's Reynolds number and the flow pattern within the reaction compartment. Because of the complex flow pattern, higher shearing forces acting on the particles and high velocity of the solid particles within the reaction compartment, especially at the impingement zone, the external mass-transfer resistance around the solid particles could be eliminated.

(2) It should be also noted that the overall rates of all chemical reactions including those catalyzed by enzymes are highly temperature dependent. In the specific case of the glucose isomerization reaction, the dependency of the apparent rate constant of the chemical reaction on temperature was reported by many investigators (see for example, Eqs. 10–13).

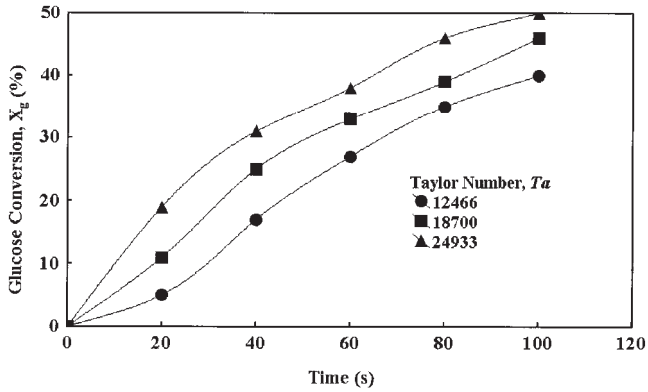

Figure 10. Effect of Taylor number (Ta) on the fractional conversion of D-glucose to D-fructose in the TIJR.

Re_{ax} = 1880; W_s = 1 g/s; standard deviations of the data points are between 1.3 and 1.5.

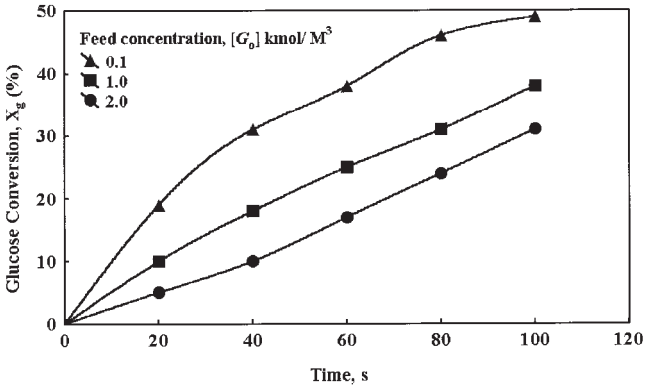

Figure 11. Effect of feed concentration [G_0] on the fractional conversion of D-glucose to D-fructose in the TIJR.

Re_{ax} = 1880; Ta = 24,933; W_s = 1 g/s; standard deviations of the data points are between 1.3 and 1.5.

Typical data concerning the glucose isomerization reaction show that the apparent rate constants of the chemical reaction are increased by a factor of 1.2–2.5 for an increase of 10°C in temperature. According to the latter, the energy released and dissipated as the result of strong collisions of the impinging jets with high velocities, recirculation of the feed solution during the operating time, and the energy dissipated as a result of the inner rotating cylinder within the reaction compartment may contribute to the total energy of the reacting system and could conceivably increase the temperature of the process, and thus may improve the external mass-transfer resistance.

Effect of the Feed Concentration, [G_0]. A number of experimental runs were carried out to investigate the effect of the feed concentration on the fractional conversion of D-glucose to D-fructose. Figure 11 illustrates the variation of the fractional conversion of D-glucose to D-fructose vs. operating time with the concentration of the feed solution [G_0], as a parameter at the mass-flow rate of the IGI enzyme particles W_s = 1 g/s, Re_{ax} = 1880, and Ta = 24,933. As may be observed, an increase in the concentration of the feed solution leads to a decrease in the fractional conversion of D-glucose measured at the same operating time. Explanations for such a decrease are presented as follows: as it is well known, the concentration of the substrate solution has a direct influence on the viscosity of the substrate solution. The molecular diffusivity, on the other hand, is proportional to the reciprocal of the viscosity at a fixed temperature, such that in most liquid solutions the following relationship holds:

$$\frac{D\mu}{T} = \text{constant} \tag{35}$$

where D, μ, and T are molecular diffusivity of the solute, viscosity, and temperature, respectively. It is highly expected that an increase in the concentration of the substrate solution causes an increase in the viscosity, consequently resulting in a decrease of the molecular diffusivity or effective diffusivity. The latter, in turn, decreases the mass-transfer rates inside and outside of the solid enzyme particles and thus decreases the fractional conversion of D-glucose. In addition, if the relative rates of the chemical reaction are extracted from these experimental results, it may be noticed that the experimental rate of chemical reaction increases with increasing feed concentration up to at least 1 kmol m^{-3} but a further increase in the feed concentration causes a decreasing rate of the chemical reaction, which occurs because, in the high concentrations of substrate solution, there is more feed to convert.

Linear Approximation of the Rate Equation. It is convenient to rewrite Eq. 7 in the following form:

$$R = k_i([G] - [G_e]) \tag{36}$$

Parameter k_i, which essentially represents a rate kinetic constant for D-glucose isomerization, and is in general a function of [G], [G_0], and T, can be split up as follows[6]:

$$k_i = k_i'(T)k_i''([G], [G_0], T) \tag{37}$$

where

$$k_i' = \frac{K_e + 1}{K_e}\frac{v_{mf}}{k_{mf}} \tag{38}$$

$$k_i'' = \frac{1}{1 + \zeta[G_0]} \tag{39}$$

$$\zeta = k_{mf}^{-1} - \varphi\left(1 - \frac{[G]}{[G_0]}\right) = \zeta([G], [G_0], T) \tag{40}$$

$$\varphi = k_{mf}^{-1} - k_{mr}^{-1} \tag{41}$$

$$[G_e] = \frac{[G_0]}{1 + K_e} \tag{42}$$

As may be seen, parameter ζ is a function of [G], which varies from [G_0] to [G_e]. In the present study, we used a mean value of ζ over the range of [G] = [G_0] =0.1 kmol m^{-3} to [G] = [G_e] = 0.05 kmol m^{-3}, that is,

$$\zeta_{mean} = \frac{\zeta([G] = [G_0]) + \zeta([G] = [G_e])}{2} \tag{43}$$

The following data for the isomerization reaction using Sweetzyme T® as IGI enzyme at 60°C have been reported by Palazzi and Converti[6]: K_e = 0.982; $k_i''(\zeta = \zeta_{mean})$ = 0.861; k_i' = 0.817 h^{-1}; and ζ_{mean} = 1.616 m^3/kmol.

Thus, Eq. 36 yields the following apparent overall rate of chemical reaction:

$$R = 0.703([G] - [G_e]) \qquad \text{mol m}^{-3}\,\text{h}^{-1} \tag{44}$$

Now, we can calculate the fractional conversion of glucose using the RTD and the linear reaction rate (Eq. 44). The concentration of glucose after the first pass of reactants from the reactor may be calculated as follows:

Table 2. Experimental and Estimated Values for the Fractional Conversion of D-Glucose in the TIJR

	Fractional Conversion (%)	
Number of Passes	Obtained	Estimated
7	20	2.22
13	30	2.89
20	37	3.67
27	43	4.44
33	49	5.1

$$C_g = \int_{t=0}^{t=\infty} C_g(t)\Xi dt \tag{45}$$

where C_g is the glucose concentration in the effluent; $C_g(t)$ is the glucose concentration remaining in an element of age t within the reactor, Ξ is the RTD function, and t is time. From Eqs. 44 and 45 we have

$$\frac{C_g(t)}{C_{g0}} = \frac{1}{2}\,(1 + e^{-0.703t}) \tag{46}$$

$$1 - X_g = \frac{1}{2}\int_{t=0}^{t=\infty} (1 + e^{-0.703t})\Xi dt \tag{47}$$

or

$$1 - X_g = \frac{1}{2}\sum_i (1 + e^{-0.703t_i})\Xi_i \Delta t_i \tag{48}$$

where X_g is the fractional conversion of glucose and t is in h.

Thus, the fractional conversion of glucose after z passes (X_{gz}) may be calculated from the following relation:

$$1 - X_{gz} = \sum_z \sum_i (1 - X_{g,i})\Xi_{i,z}\Delta t_i \tag{49}$$

The number of passes (z) was found by dividing the total reaction time by the mean residence time of the reaction system. Thus, the duration of each pass is approximately equal to the mean residence time of the reactor. Table 2 shows that the estimated and experimental values of the fractional conversion of D-glucose differ significantly. An explanation for the much lower values of the estimated fractional conversion of D-glucose by using the apparent rate constant is that the overall rate of the reaction carried out under conventional conditions is not governed just by the intrinsic rate of reaction. In other words, the overall rate of reaction may be affected by both internal (pore diffusion) and external mass-transfer resistances. Thus, in such a case the apparent rate constant (literature rate constant) k_i accounts for both external and internal mass-transfer and kinetic effects. In the novel TIJR the external mass-transfer resistance of the liquid film surrounding the IGI particles is low because of the high velocity of the particles within the TIJR. These explanations clearly were supported by the experimental results presented in Table 1, which shows that the fractional conversions of the glucose in the conventional reaction systems were severely affected by the external mass-transfer limitations.

Conclusions

A novel type of TIJR was used as a chemical reactor for solid–liquid enzyme reactions using the isomerization of glucose to fructose as a typical model system. Some aspects of hydrodynamic behavior of the TIJR were investigated within a range of operating conditions such as axial Reynolds number, Taylor number, feed concentration, and solid-mass flow rate. The RTD of solid particles within the reactor was determined using tracer analysis. A Markov chains model with two parameters was proposed to comply with the flow pattern in the reactor. The parameters of the model were evaluated and adjusted using experimental RTD data.

From the experimental results, it was observed that the fractional conversion of glucose in the TIJR was much higher than that obtained in conventional reactors such as batch stirred tank reactors and packed-bed reactors. This may be attributed to the elimination of the external mass-transfer resistances around the solid particles, complex flow pattern within the reactor, and energy released as the result of impinging-jets collision, energy dissipated in the annular gap, and high intensity mixing at the impingement zone.

Acknowledgments

The author thanks Mohammad Mehdi Ghafari for help and participation in the experimental work and gratefully acknowledges Novo Nordisk for providing IGI.

Notation

C_g = concentration of glucose, kmol/m^3
C_{g0} = initial concentration of glucose, kmol/m^3
C_i = number of painted particle (concentration) corresponding to a specific experiment i
C_m = mean number (concentration) of tagged particle, Eq. 17
d = annular space width = $R_o - R_i$, m
E = enzyme
$[E]$ = concentration of enzyme, kmol/m^3
$[E_t]$ = total amount of enzyme, kmol/m^3
F = D-fructose
$[F]$ = concentration of fructose, kmol/m^3
G = D-glucose
$[G]$ = concentration of glucose, kmol/m^3
K_e = equilibrium constant, Eq. 6
k_f = rate constant, Eq. 1
k_{-f} = rate constant, Eq. 1
k_g = rate constant, Eq. 1
k_{-g} = rate constant, Eq. 1
k_i = linearized reaction rate constant, Eq. 36
k_i' = rate constant, Eq. 38
k_i' = rate constant, Eq. 39
K_m = constant, Eq. 9
K_{mf} = Michaelis–Menten constant for forward reaction, Eq. 4
K_{mr} = Michaelis–Menten constant for reverse reaction, Eq. 4
m = number of repetitive experiments
N = number of states
n = number of transition
n_v = number of vessels
p_{ij} = transition probability
$\mathbf{P}$ = transition matrix, Eq. 22
r = solid recycle stream mass flow rate, g/s
r_r = solid recycle stream ratio, Eq. 26
R = reaction rate of glucose, Eq. 2

Re_{ax} = axial Reynolds number, Eq. 14
R_i = inner cylinder radius, m
R_o = outer radius of annular space, m
$s_i(n)$ = state probability
$\mathbf{S}(0)$ = initial state probability vector, Eq. 28
$\mathbf{S}(n)$ = state probability vector
T = temperature, K
Ta = Taylor number, Eq. 15
t = time, s
t_m = mean residence time, s
U_{ax} = mean axial velocity, m/s
v_m = constant, Eq. 8
v_{mf} = maximum velocity for forward reaction, Eq. 4
v_{mr} = maximum velocity for reverse reaction, Eq. 4
W_s = mass-flow rate of solid particles, g/s
W_1 = liquid mass-flow rate, g/s
X = intermediate complex, Eq. 1
X_g = fractional conversion of glucose
X_{gz} = fractional conversion of glucose after z passes, Eq. 49
$[X]$ = concentration of intermediate complex, kmol/m^3
z = number of passes

Greek letters

α = constant, Eq. 24
β = constant, Eq. 25
ν = kinematic viscosity, m^2/s
θ = dimensionless time = t/t_m, Eq. 27
σ^2 = variance, s^2
Δ = difference operator
ω = inner rotating cylinder speed, rev/s
φ = parameter, Eq. 41
ζ = parameter, Eq. 40
ψ = holdup
μ = viscosity
Ξ = RTD function

Subscripts

e = at equilibrium
exp = experimental
l = liquid
mod = model
0 = initial concentration
s = solid

Abbreviations

BSTR = batch stirred tank reactor
CSTR = continuous stirred tank reactor
DC = drain connection
DJR = down flow jet reactor
IE = immobilized enzyme
IJ = impinging jets
IGI = immobilized glucose isomerase
PBR = packed-bed reactor
PHI = pH meter
PI = pressure indicator
RTD = residence time distribution
SC = sampling connection
TI = temperature indicator
TIJ = two impinging jets
TIJR = two-impinging-jets reactor

Literature Cited

1. Vilonen KM, Vuolanto A, Jokela J, Leisola MSA, Krause AOI. Enhanced glucose to fructose conversion in acetone with xylose isomerase stabilized by crystallization and cross-linking. *Biotechnol Prog.* 2004;20:1555-1560.
2. Toumi A, Engell S. Optimization-based control of a reactive simulated moving bed process for glucose isomerization. *Chem Eng Sci.* 2004; 59:3777-3792.
3. Zhang Y, Hidajat K, Ray AK. Optimal design and operation of SMB bioreactor: Production of high fructose syrup by isomerization of glucose. *Biochem Eng J.* 2004;21:111-121.
4. Faqir NM, Attarakih MM. Optimal temperature policy for immobilized enzyme packed bed reactor performing reversible Michaelis–Menten kinetics using the disjoint policy. *Biotechnol Bioeng.* 2002; 77:163-173.
5. Palazzi E, Converti A. Evaluation of diffusional resistances in the process of glucose isomerization to fructose by immobilized glucose isomerase. *Enzyme Microb Technol.* 2001;28:246-252.
6. Palazzi E, Converti A. Generalized linearization of kinetics of glucose isomerization to fructose by immobilized glucose isomerase. *Biotechnol Bioeng.* 1999;63:273-284.
7. Lee HS, Hong J. Kinetics of glucose isomerization to fructose by immobilized glucose isomerase: Anomeric reactivity of D-glucose in kinetic model. *J Biotechnol.* 2000;84:145-153.
8. Asif M, Abasaeed AE. Modeling of glucose isomerization in a fluidized bed immobilized enzyme bioreactor. *Bioresour Technol.* 1998; 64:229-235.
9. Bravo V, Jurado E, Luzon G, Cruz N. Kinetics of fructose–glucose isomerization with Sweetzyme type A. *Can J Chem Eng.* 1998;76: 778-783.
10. Straatsma J, Vellenga K, de Willt HGJ, Joosten GEH. Isomerization of glucose to fructose. 1. The stability of a whole cell immobilized glucose isomerase catalyst. *Ind Eng Chem Process Des Dev.* 1983;22: 349-356.
11. Straatsma J, Vellenga K, de Willt HGJ, Joosten GEH. Isomerization of glucose to fructose. 2. Optimization of reaction conditions in the production of high fructose syrup by isomerization of glucose catalyzed by a whole cell immobilized glucose isomerase catalyst. *Ind Eng Chem Process Des Dev.* 1983;22:356-361.
12. Messing RA, Filbert AM. An immobilized glucose isomerase for the continuous conversion of glucose to fructose. *J Agric Food Chem.* 1975;23:920-923.
13. Haas WR, Tavlarides LL, Wnek W. Optimal temperature policy for reversible reactions with deactivation: Applied to enzyme reactors. *AIChE J.* 1974;20:707-712.
14. Bailey JE, Ollis DF. *Biochemical Engineering Fundamentals*. 2nd Edition. New York, NY: McGraw-Hill; 1986.
15. Carver JA, Plains S, Rollman WF. *Method and Apparatus for Mixing and Contacting Fluids*. U.S. Patent No. 2 751 335; 1956.
16. Elperin IT. Heat and mass transfer in opposing currents (in Russian). *J Eng Phys.* 1961;6:62-68.
17. Tamir A. *Impinging Streams Reactors: Fundamentals and Applications*. Amsterdam, The Netherlands: Elsevier; 1994.
18. Hosseinalipour SM, Mujumdar AS. Flow and thermal characteristics of steady two-dimensional confined laminar opposing jets: I. Equal jets. *Int Commun Heat Mass Transfer.* 1997;24:27-38.
19. Hosseinalipour SM, Mujumdar AS. Flow and thermal characteristics of steady two-dimensional confined laminar opposing jets: II. Unequal jets. *Int Commun Heat Mass Transfer.* 1997;24:39-50.
20. Hosseinalipour SM, Mujumdar AS. Comparative evaluation of different turbulence models for confined impinging and opposing jet flows. *Numer Heat Transfer A Appl.* 1995;28:647-666.
21. Seyedein SH, Hasan M, Mujumdar AS. Modeling of a single confined turbulent slot jet impingement using various k–ε turbulence models. *Appl Math Model.* 1994;18:526-537.
22. Herskowits D, Herskowits V, Tamir A. Desorption of acetone in a two-impinging-streams spray desorber. *Chem Eng Sci.* 1987;42:2331-2337.
23. Tamir A, Herskowits D, Herskowits V. Impinging-jets absorber. *Chem Eng Process.* 1990;28:165-172.
24. Tamir A, Herskowits D, Herskowits V, Stephen K. Two-impinging jets absorber. *Ind Eng Chem Res.* 1990;29:272-277.
25. Herskowits D, Herskowits V, Stephen K, Tamir A. Characterization of a two-phase impinging jet absorber: I. Physical absorption of CO_2 in water. *Chem Eng Sci.* 1988;43:2773-2780.
26. Kleingeld AW, Lorenzen L, Botes FG. The development and modeling of high-intensity impinging streams jet reactors for effective mass transfer in heterogeneous systems. *Chem Eng Sci.* 1999;54:4991-4995.
27. Tamir A, Grinholtz M. Performance of a continuous solid–liquid two-impinging streams (TIS) reactor: Dissolution of solids, hydrodynamics, mean residence time and holdup of the particles. *Ind Eng Chem Res.* 1987;26:726-731.

28. Kitron Y, Tamir A. Performance of a coaxial gas–solid two-impinging-streams (TIS) reactor: Hydrodynamics, residence time distribution, and drying heat transfer. *Ind Eng Chem Res.* 1988;27:1760-1767.
29. Kudra T, Mujumdar AS. Impinging streams dryers for particles and pastes. *Drying Technol.* 1989;7:219-266.
30. Kudra T, Mujumdar AS. Impinging stream dryers. In: Mujumdar AS, ed. *Handbook of Industrial Drying*. 2nd Edition. New York, NY: Marcel Dekker; 1995.
31. Kudra T, Mujumdar AS, Meltser VL. *Impinging Stream Dryers; Principles, Practice and Potential: Drying of Solids*. Meerut, India: Sarita Prakashan; 1991.
32. Hosseinalipour SM, Mujumdar AS. Superheated steam drying of a single particle in an impinging streams dryer. *Drying Technol.* 1995; 13:1279-1303.
33. Berman Y, Tamir A. Experimental investigation of phosphate dust collection in impinging streams (IS). *Can J Chem Eng.* 1996;74:817-821.
34. Herskowits D, Herskowits V, Stephen K, Tamir A. Characterization of a two-phase impinging jet absorber: II. Absorption with chemical reaction of CO_2 in NaOH solutions. *Chem Eng Sci.* 1990;45:1281-1287.
35. Sohrabi M, Jamshidi AM. Studies on the behavior and application of the continuous two-impinging streams reactors in gas–liquid reactions. *J Chem Technol Biotechnol.* 1997;69:415-420.
36. Sohrabi M, Kaghazchi T, Yazdani F. Modeling and the application of the continuous impinging streams reactors in liquid–liquid heterogeneous reactions. *J Chem Technol Biotechnol.* 1993;58:363-370.
37. Unger DR, Muzzio FJ, Brodkey RS. Experimental and numerical characterization of viscous flow and mixing in an impinging jet contactor. *Can J Chem Eng.* 1998;76:546-555.
38. Devahastin S, Mujumdar AS. A numerical study of flow and mixing characteristics of laminar confined impinging streams. *Chem Eng J.* 2002;85:215-223.
39. Devahastin S, Mujumdar AS. A numerical study of mixing in a novel impinging stream inline mixer. *Chem Eng Process.* 2001;40:459-470.
40. Devahastin S, Mujumdar AS. A study of turbulent mixing of confined impinging stream using a new composite turbulence model. *Ind Eng Chem Res.* 2001;40:4998-5004.
41. Yao B, Berman Y, Tamir A. Evaporative cooling of air in impinging streams. *AIChE J.* 1995;41:1667-1675.
42. Sievers M, Gaddis ES, Vogelpohl A. Fluid dynamics in an impinging-streams reactor. *Chem Eng Process.* 1995;34:115-119.
43. Sohrabi M, Marvast MA. Application of a continuous two impinging streams reactor in solid–liquid enzyme reactions. *Ind Eng Chem Res.* 2000;39:1903-1910.
44. Berman Y, Tamir A. Extraction in thin liquid films generated by impinging streams. *AIChE J.* 2000;46:769-778.
45. Dehkordi AM, Kaghazchi T, Sohrabi M. Application of an air-operated two impinging streams extractor in liquid–liquid extraction and comparison with other contactor types. *Can J Chem Eng.* 2001;79: 227-235.
46. Dehkordi AM. Novel type of impinging streams contactor for liquid–liquid extraction. *Ind Eng Chem Res.* 2001;40:681-688.
47. Dehkordi AM. A novel two-impinging-jets reactor for copper extraction and stripping processes. *Chem Eng J.* 2002;87:227-238.
48. Dehkordi AM. Experimental investigation of an air-operated two-impinging-streams reactor for copper extraction processes. *Ind Eng Chem Res.* 2002;41:2512-2520.
49. Dehkordi AM. Liquid–liquid reaction with chemical reaction in a novel impinging-jets reactor. *AIChE J.* 2002;48:2230-2239.
50. Dehkordi AM. Liquid–liquid extraction with an interphase chemical reaction in an air-driven-two-impinging-streams reactor: Effective interfacial area and overall mass-transfer coefficient. *Ind Eng Chem Res.* 2002;41:4085-4093.
51. Johnson BK, Prudhomme RK. Chemical processing and micromixing in confined impinging jets. *AIChE J.* 2003;49:2264-2282.
52. Mahajan AJ, Kirwan DJ. Micromixing effect in a two-impinging-jets precipitator. *AIChE J.* 1996;42:1801-1814.
53. Hacherl JM, Paul EL, Buettner HM. Investigation of impinging-jet crystallization with a calcium oxalate model system. *AIChE J.* 2003; 49:2352-2362.
54. Chen KC, Wu JY. Substrate protection of immobilized glucose isomerase. *Biotechnol Bioeng.* 1987;30:817-824.
55. Roels JA. *Energetics and Kinetics in Biotechnology*. Amsterdam, The Netherlands: Elsevier; 1983.
56. Camacho-Rubio F, Jurado-Alameda E, Gonzalez-Tello P, Luzon-Gonzaez G. Kinetic study of fructose–glucose isomerization in a recirculation reactor. *Can J Chem Eng.* 1995;73:935-940.
57. Coburn HJ, Carrol JJ. Improved manual and automated colorimetric determination of serum glucose, with use of hexokinase and glucose-6-phosphate dehydrogenase. *Clin Chem.* 1973;19:127-130.
58. Dische Z, Borenfreund E. A new spectrophotometric method for the detection and determination of keto sugar and trioses. *J Biol Chem.* 1951;192:583–587.
59. Salehi Z, Sohrabi M, Kaghazchi T, Bonakdarpour B. Application of down flow jet loop bioreactors in implementation and kinetic determination of solid–liquid enzyme reactions. *Process Biochem.* 2005; 40:2455-2460.
60. Giordano RC, Giordano RLC, Prazeres DMF, Cooney CL. Analysis of a Taylor–Poieuille vortex flow reactor—I: Flow patterns and mass transfer characteristics. *Chem Eng Sci.* 1998;53:3635-3652.
61. Van de Vusse JG. A new model for the stirred tank reactor. *Chem Eng Sci.* 1962;17:507-521.
62. Tamir A. *Application of Markov Chains in Chemical Engineering*. Amsterdam, The Netherlands: Elsevier; 1998.
63. Benaiges MD, Sola C, deMas C. Intrinsic kinetic constants of an immobilized glucose-isomerase. *J Chem Technol Biotechnol.* 1986;36: 480-486.

Manuscript received Jan. 1, 2005, and revision received July 24, 2005.